Inorg. Chem. **2009**, *48*, 82−89

A Cobalt(II) Hexafluoroacetylacetonate Ethylenediamine Complex As a CVD Molecular Source of Cobalt Oxide Nanostructures

Giuliano Bandoli,[†] Davide Barreca,[*,‡] Alberto Gasparotto,[§] Chiara Maccato,[§] Roberta Seraglia,[‡] Eugenio Tondello,[§] Anjana Devi,[||] Roland A. Fischer,[||] and Manuela Winter[||]

Department of Pharmaceutical Sciences, Padova University, 35131 Padova, Italy, ISTM-CNR and INSTM, Department of Chemistry, Padova University, 35131 Padova, Italy, Department of Chemistry, Padova University and INSTM, Via Marzolo, 1, 35131 Padova, Italy, Inorganic Materials Chemistry Group, Lehrstuhl für Anorganische Chemie II, Ruhr-University Bochum, D-44780 Bochum, Germany

Received July 1, 2008

An adduct of Co(II) 1,1,1,5,5,5-hexafluoro-2,4-pentanedionate with *N,N,N′,N′*-tetramethylethylenediamine is synthesized by a simple procedure and, for the first time, thoroughly characterized by several analytical methods in order to elucidate its structure (single-crystal X-ray diffraction), chemical composition (elemental analyses, FT-IR), optical properties (UV−vis absorption spectroscopy), thermal behavior (thermogravimetric analysis and differential scanning calorimetry), and fragmentation pathways (electrospray ionization mass spectrometry and tandem mass spectrometry). The target complex is monomeric with a *pseudo*-octahedral Co(II) core and presents a clean decomposition pathway and a high volatility at moderate temperatures. Preliminary chemical vapor deposition (CVD) experiments highlight its very promising features as a CVD/atomic layer deposition molecular source for cobalt oxide nanosystems.

Introduction

The attractive properties of cobalt oxide (CoO, Co_3O_4) nanosystems, such as high catalytic activity,[1,2] antiferromagnetism,[3] and electrochromism,[4] offer significant potential in view of various technological applications. As a matter of fact, both CoO and Co_3O_4 nanosystems are promising candidates for use in thermal solar energy conversion devices,[5−7] electrochemical capacitors,[8,9] solid-state gas sensors,[10,11] magnetic materials,[12,13] and negative electrodes for lithium-ion batteries.[14−17]

In the past decade, this broad spectrum of attractive utilization has stimulated widespread research efforts aimed at the synthesis of Co−O thin films, nanotubes, and ordered nanoarrays, as summarized by various reports.[6,7,10,12,18] Among the different proposed routes, chemical vapor deposition (CVD) and atomic layer deposition (ALD)

* Author to whom correspondence should be addressed. Tel.: + 39 049 8275170. Fax: + 39 049 8275161. E-mail: davide.barreca@unipd.it.
† Department of Pharmaceutical Sciences, Padova University.
‡ ISTM-CNR and INSTM.
§ Department of Chemistry, Padova University and INSTM.
|| Ruhr-University Bochum.

(1) Pollard, M. J.; Weinstock, B. A.; Bitterwolf, T. E.; Griffiths, P. R.; Newbery, A. P.; Paine, J. B. *J. Catal.* **2008**, *254*, 218.
(2) Yang, Q. J.; Choi, H.; Dionysiou, D. D. *Appl. Catal., B* **2007**, *74*, 170.
(3) Ikedo, Y.; Sugiyama, J.; Nozaki, H.; Itahara, H.; Brewer, J. H.; Ansaldo, E. J.; Morris, G. D.; Andreica, D.; Amato, A. *Phys. Rev. B: Condens. Matter.* **2007**, *75*, 054424.
(4) Granqvist, C. G. *Handbook of Inorganic Electrochromic Materials*; Elsevier: Amsterdam, 1995.
(5) Gulino, A.; Dapporto, P.; Rossi, P.; Fragalà, I. *Chem. Mater.* **2003**, *15*, 3748.
(6) Gulino, A.; Fiorito, G.; Fragalà, I. *J. Mater. Chem.* **2003**, *13*, 861.
(7) Gulino, A.; Dapporto, P.; Rossi, P.; Anastasi, G.; Fragalà, I. *J. Mater. Chem.* **2004**, *14*, 2549.
(8) Shinde, V. R.; Mahadik, S. B.; Gujar, T. P.; Lokhande, C. D. *Appl. Surf. Sci.* **2006**, *252*, 7487.
(9) Armelao, L.; Barreca, D.; Gross, S.; Martucci, A.; Tieto, M.; Tondello, E. *J. Non-Cryst. Solids* **2001**, *293−295*, 477.
(10) Barreca, D.; Massignan, C.; Daolio, S.; Fabrizio, M.; Piccirillo, C.; Armelao, L.; Tondello, E. *Chem. Mater.* **2001**, *13*, 588.
(11) Pasko, S.; Hubert-Pfalzgraf, L. G.; Abrutis, A.; Vaissermann, J. *Polyhedron* **2004**, *23*, 735.
(12) Pasko, S.; Abrutis, A.; Hubert-Pfalzgraf, L. G.; Kubilius, V. *J. Cryst. Growth* **2004**, *262*, 653.
(13) Verelst, M.; Ely, T. O.; Amiens, C.; Snoeck, E.; Lecante, P.; Mosset, A.; Respaud, M.; Broto, J. M.; Chaudret, B. *Chem. Mater.* **1999**, *11*, 2702.
(14) Poizot, P.; Laruelle, S.; Grugeon, S.; Dupont, L.; Tarascon, J.-M. *Nature* **2000**, *407*, 496.
(15) Tarascon, J.-M.; Grugeon, S.; Morcrette, M.; Laruelle, S.; Rozier, P.; Poizot, P. *C. R. Chimie* **2005**, *8*, 9.
(16) Poizot, P.; Laruelle, S.; Grugeon, S.; Dupont, L.; Tarascon, J.-M. *J. Power Sources* **2001**, *97−98*, 235.
(17) Jiang, C.; Hosono, E.; Zhou, H. *NanoToday* **2006**, *1*, 28.
(18) Klepper, K. B.; Nilsen, O.; Fjellvåg, H. *Thin Solid Films* **2007**, *515*, 7772.

10.1021/ic801212v CCC: $40.75
Published on Web 12/02/2008

represent preferred techniques for the growth of high-quality nanoarchitectures.[19] Yet, the success of a CVD/ALD process depends critically on the availability of volatile and thermally stable precursors, enabling uniform and reproducible growth processes along with a tailoring of the system properties. In this regard, several cobalt(II) and (III) salts have been proposed, such as CoI_2, $Co(OCOCH_3)_2$, and $Co(NO_3)_3$,[10−12,20] but they do not present a sufficiently controlled and reproducible mass supply. Alternatively, cobalt complexes such as $Co_2(CO)_8$, $Co(C_5H_5)_2$, and related organometallic species, including $Co(CO)_3NO$, $HCo(CO)_4$, and $Co(C_5H_5)(CO)_2$, have also been adopted as CVD precursors, but their use presents serious drawbacks, such as undesired gas-phase reactions, low thermal stability, and a high deposition temperature.[21−27] Other works have focused on the use of conventional Co β-diketonates as CVD/ALD precursors, such as $Co(acac)_2$ (acac = 2,4-pentanedionate) and $Co(dpm)_2$ (dpm = 2,2,6,6-tetramethyl-3,5-heptanedionate).[10,28,29] Unfortunately, the former is characterized by the formation of oligomeric structures.[11] Although such phenomena can be limited by increasing the steric hindrance of the ligand, for instance, upon going to $Co(dpm)_2$, the latter compound suffers from sintering at elevated temperatures and presents a limited shelf life. In fact, the structure of bis(β-diketonato)Co(II) chelates was long clouded by ambiguity, due to the pronounced tendency of Co(II) to achieve six-coordination through adduct formation.[30] As a consequence, the development of improved Co(II) β-diketonate sources actually remains an open challenge in this field.

Recently, the syntheses of $Co(hfa)_2 \cdot 2H_2O$ and $Co(hfa)_2 \cdot 2H_2O \cdot L$ adducts [L = bis(2-methoxyethyl)ether, 2,5,8,11-tetraoxadodecane, and 2,5,8,11,14-pentaoxapentadecane] have been reported.[5,6,31] Although the properties of these precursors compare favorably with those of conventional β-diketonates, water molecules in the metal coordination sphere might induce uncontrolled decomposition or premature reactions in CVD/ALD processes.

An attractive alternative is the formation of adducts between Co(II) β-diketonates and various *N*-donor Lewis bases,[11,30,32] which enables a complete saturation of the Co(II) coordination sphere, thus resulting in stable adducts with improved properties. Recently, $Co(acac)_2$ and $Co(dpm)_2$ adducts with *N*,*N*,*N*′,*N*′-tetramethylethylenediamine (TMEDA) and 1-dimethylamino-2-propanol (DMAPH) have been proposed as CVD precursors.[11,12] While the latter is dimeric, Co(II)-TMEDA adducts present better resistance to air oxidation than the parent Co(II) β-diketonates,[11] implying higher stability and a longer shelf life, significant advantages for large-scale CVD/ALD applications.

In the past decade, various $M(hfa)_x \cdot$TMEDA complexes (x = 1, 2; e.g., M = Mg(II),[33] Ag(I),[34] Zn(II)[35−37] and Cd(II)[38,39] compounds) have come under intense scrutiny thanks to their favorable properties as CVD/ALD precursors to metal and metal oxide films. In fact, the introduction of fluorinated substituents (e.g., hfa versus acac) effectively increases both the precursor volatility and the stability of ancillary amine ligand binding via enhanced Lewis acidity.[35] On this basis, in the present work, our attention was focused on an innovative Co(II) compound, $Co(hfa)_2 \cdot$TMEDA, appealing as a potential CVD/ALD precursor of Co−O nanosystems. To the best of our knowledge, only a previous patent quoting the use of such a compound and of its Mn, Fe, and Ni homologues as gasoline additives is available,[40] but no reports on its synthesis, characterization, and use are available in the literature to date.

In this paper, the target compound was prepared and fully characterized with particular attention to its mass-transport properties and reactivity, two critical issues for CVD/ALD applications. The functional validation of the precursor has also been established by performing preliminary Co−O CVD depositions on Si(100) substrates.

Experimental Section

Reagents. $CoCl_2 \cdot 6H_2O$ (98%) was purchased from Prolabo-Rectapur. The chemical reagents Hhfa (98+%, d = 1.47 g mL^{-1}) and TMEDA (99%, d = 0.77 g mL^{-1}) were commercial products obtained from Alfa Aesar and Janssen, respectively. All of the above products were used as received without any further purification.

General Procedures. Elemental microanalyses were performed using a Fisons Carlo Erba EA1108 instrument, CHNS version. The

(19) Hitchman, M. L.; Jensen, K. F. *Chemical Vapor Deposition: Principles and Applications*; Academic Press: London, 1993.
(20) Rooth, M.; Lindahl, E.; Harsta, A. *Chem. Vapor Deposition* **2006**, *12*, 209.
(21) Crawford, N. R. M.; Knutsen, J. S.; Yang, K. A.; Haugstad, G.; McKernan, S.; McCormick, F. B.; Gladfelter, W. L. *Chem. Vapor Deposition* **1998**, *4*, 181.
(22) Lane, P. A.; Oliver, P. E.; Wright, P. J.; Reeves, C. L.; Pitt, A. D.; Cockayne, B. *Chem. Vapor Deposition* **1998**, *4*, 183.
(23) Holgado, J. P.; Caballero, A.; Espinós, J. P.; Morales, J.; Jiménez, V. M.; Justo, A.; González-Elipe, A. R. *Thin Solid Films* **2000**, *377−378*, 460.
(24) Choi, H.; Park, S. *Chem. Mater.* **2003**, *15*, 3121.
(25) Tyczkowski, J.; Kapica, R.; Łojewska, J. *Thin Solid Films* **2007**, *515*, 6590.
(26) Daub, M.; Knez, M.; Goesele, U.; Nielsch, K. *J. Appl. Phys.* **2007**, *101*, 09J111.
(27) Li, Z.; Lee, D. K.; Coulter, M.; Rodriguez, L. N. J.; Gordon, R. G. *Dalton Trans.* **2008**, *19*, 2592.
(28) Barison, S.; Barreca, D.; Daolio, S.; Fabrizio, M.; Tondello, E. *Rapid Commun. Mass Spectrom.* **2001**, *15*, 1621.
(29) Klepper, K. B.; Nilsen, O.; Fjellvåg, H. *J. Cryst. Growth* **2007**, *307*, 457.
(30) Tzavellas, L. C.; Tsiamis, C.; Kavounis, C. A.; Cardin, C. J. *Inorg. Chim. Acta* **1997**, *262*, 53.
(31) Gulino, A.; Fragalà, I. *Inorg. Chim. Acta* **2005**, *358*, 4466.
(32) Colborn, R. E.; Garbauskas, M. F.; Hejna, C. I. *Inorg. Chem.* **1988**, *27*, 3661.
(33) Wang, L.; Yang, Y.; Ni, J.; Stern, C. L.; Marks, T. J. *Chem. Mater.* **2005**, *17*, 5697.
(34) Zanotto, L.; Benetollo, F.; Natali, M.; Rossetto, G.; Zanella, P.; Kaciulis, S.; Mezzi, A. *Chem. Vapor Deposition* **2004**, *10*, 207.
(35) Ni, J.; Yan, H.; Wang, A.; Yang, Y.; Stern, C. L.; Metz, A. W.; Jin, S.; Wang, L.; Marks, T. J.; Ireland, J. R.; Kannewurf, C. R. *J. Am. Chem. Soc.* **2005**, *127*, 5613.
(36) Barreca, D.; Ferrucci, A. P.; Gasparotto, A.; Maccato, C.; Maragno, C.; Tondello, E. *Chem. Vapor Deposition* **2007**, *13*, 618.
(37) Barreca, D.; Comini, E.; Ferrucci, A. P.; Gasparotto, A.; Maccato, C.; Maragno, C.; Sberveglieri, G.; Tondello, E. *Chem. Mater.* **2007**, *19*, 5642.
(38) Babcock, J. R.; Wang, A. C.; Metz, A. W.; Edleman, N. L.; Metz, M. V.; Lane, M. A.; Kannewurf, C. R.; Marks, T. J. *Chem. Vapor Deposition* **2001**, *7*, 239.
(39) Metz, A. W.; Lane, M. A.; Kannewurf, C. R.; Poeppelmeier, K. R.; Marks, T. J. *Chem. Vapor Deposition* **2004**, *10*, 207.
(40) McCormack, W. B.; Sandy, C. A. Patent Ger. Offen. DE 292095, 1979; U.S. 78-907875, 1978.

complex melting point was measured in the air by means of a Koffler microscope. FT-IR analyses were performed on KBr pellets in transmittance mode by means of a Thermo-Nicolet Nexus 860 spectrophotometer, using a spectral resolution of 4 cm^{-1}. Optical absorption analyses were performed in 2×10^{-4} M ethanolic solutions using a Cary 5000 UV−vis-NIR spectrophotometer (Varian) with a spectral bandwidth of 1 nm. Measurements were carried out on ethanolic solutions using quartz cuvettes (optical path = 1 cm). Thermal analyses were performed using an SDT 2960 apparatus from TA Instruments, which allows performance of simultaneous DSC-TGA measurements. The weight of the used sample was in the range 6−7 mg. The traces were recorded under both N_2 and synthetic air (N_2/O_2 = 80:20) flows, with a heating rate of 10 °C/min. Isothermal investigations were carried out in the air.

The ESI mass spectra were obtained using an LCQ instrument (Finnigan), operating in both positive and negative ion modes. The entrance capillary temperature and voltage were set at 200 °C and ±5 kV, respectively. 10^{-6} M solution of the target compound in methanol, methanol/water (50:50 v/v), and chloroform were introduced by direct infusion using a syringe pump at a flow rate of 8 μL/min. Accurate mass measurements were performed using an Accurate-Mass 6520 Q-TOF instrument (Agilent Technologies, Inc.), operating under ESI negative ion conditions. The solutions of $Co(hfa)_2 \cdot$TMEDA were directly injected into the Dual ESI source at a flow rate of 5 μL/min. Instrument calibration was achieved by injection of a TOF ESI Tune Mix solution (Agilent Technologies, Inc.). The mass resolution was >13.000 at *m/z* 2722.

Synthesis. 0.94 g of NaOH (23.5 mmol) were dissolved in 10 mL of deionized H_2O. Subsequently, 3.3 mL of Hhfa (23.3 mmol) was introduced in the above solution kept under stirring. To the resulting liquid was added dropwise $CoCl_2 \cdot 6H_2O$ (2.79 g, 11.73 mmol) dissolved in 50 mL of H_2O, under vigorous stirring, producing a color change from violet to orange. After 1 h, TMEDA (1.8 mL, 11.93 mmol) was dropped stepwise into the obtained solution, resulting in a color change to a brownish color. After reaction for 2.5 h, the complex was repeatedly extracted in 1,2-dichloroethane until a colorless aqueous phase was obtained. Solvent removal at reduced pressure yielded, finally, a light brown solid (yield = 60%).

Melting point: 92−94 °C at 1 atm. Anal. calcd. for $C_{16}H_{18}O_4N_2F_{12}Co$: C, 32.61%; H, 3.08%; N, 4.75%. Found: C, 32.66%; H, 3.00%; N, 4.71%.

X-Ray Crystallographic Study. A crystal having the dimensions $0.60 \times 0.50 \times 0.41$ mm^3 was used for the data collection. Crystallographic data were obtained by means of an Xcalibur 2 Oxford apparatus using graphite monochromated Mo Kα radiation (λ = 0.71073 Å, T = 107 K). The structure was solved using the SHELXL-97R software package and refined by full-matrix least-squares methods based on F^2 with all of the observed reflections.

CVD Deposition and Film Characterization. Cobalt oxide based specimens were deposited on HF-etched Si(100) substrates in an O_2 atmosphere using a cold-wall low-pressure horizontal CVD reactor equipped with a quartz tubular chamber and a resistively heated susceptor. In the present study, the precursor vaporization temperature and the deposition temperature were set at 60 and 400 °C, respectively. The pressure and gas flow rates (10 mbar and 200 sccm, respectively) were measured by a capacitance manometer (BOC Edwards) and mass-flow controllers (MKS Instruments), respectively. The deposition time was 120 min.

Glancing Incidence X-Ray Diffraction (GIXRD) patterns were recorded using a Bruker D8 Advance instrument equipped with a Göbel mirror and a Cu Kα source (40 kV, 40 mA), at an incidence angle of 0.5°. The average crystallite size was estimated by means of the Scherrer equation. X-ray photoelectron spectroscopy (XPS) and X-ray Excited Auger Electron Spectroscopy were run by a Perkin-Elmer Φ 5600ci spectrometer with a nonmonochromatized Al Kα (1486.6 eV) source, at a working pressure lower than 2×10^{-9} mbar. The reported binding energies (BEs; standard deviation= ± 0.2 eV) were corrected for charging effects, assigning to the C1s line of adventitious carbon a BE of 284.8 eV. The atomic compositions were evaluated using sensitivity factors provided by Φ V5.4A software. Ar^+ sputtering was carried out for 5 min at 3.5 kV, with an argon partial pressure of 5×10^{-8} mbar. Field emission-scanning electron microscopy (FE-SEM) and energy dispersive X-ray spectroscopy (EDXS) measurements were carried out by means of a Field Emission Zeiss SUPRA 40VP instrument, equipped with an Oxford INCA x-sight X-ray detector.

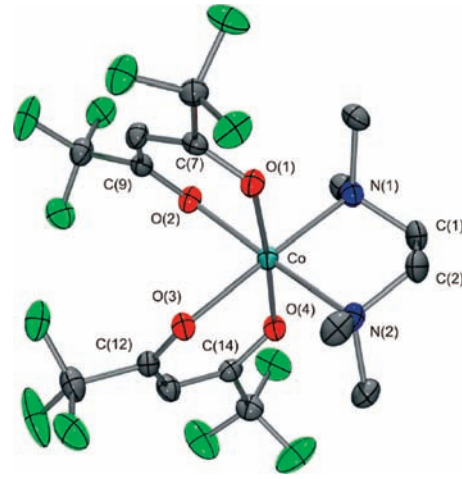

Figure 1. ORTEP view of the molecular structure of $Co(hfa)_2 \cdot$TMEDA.

Results and Discussion

Synthesis. The preparation of $Co(hfa)_2 \cdot$TMEDA was made according to the following scheme:

$$CoCl_2 \cdot 6H_2O + 2Hhfa + 2NaOH + TMEDA \rightarrow Co(hfa)_2 \cdot TMEDA + 2NaCl + 8H_2O \quad (1)$$

The above reaction is simple, straightforward, and low-cost and can be easily carried out on open benches, without the need of controlled atmospheres, thus resulting in more amenable routes than the previous ones proposed for Co(II) β-diketonate diamine adducts.[32] The Co complex can be readily dissolved in a great variety of liquids, including ethanol, acetone, CH_2Cl_2, 1,2-dichloroethane, and *n*-pentane, whereas it is insoluble in H_2O. In view of CVD applications, it is important to highlight that the resulting compound possesses a relatively low melting point (92−94 °C), is moisture- and light-stable, and has a shelf life of several months, implying that its manipulation can be readily performed in the air without inducing any undesired premature decomposition.

X-Ray Crystallographic Study of $Co(hfa)_2 \cdot$TMEDA. An ORTEP drawing of the obtained compound structure is proposed in Figure 1, while relevant crystallographic data and structural refinement parameters are summarized in Table 1. As can be seen, the target product is monomeric and

Table 1. Crystal Data and Structure Refinement for Complex $Co(hfa)_2 \cdot TMEDA$

empirical formula	$C_{16}H_{18}O_4N_2F_{12}Co$
formula weight	589.25
T (K)	107
λ (Å)	0.71073
cryst syst, space group	monoclinic, $P2_1/n$
a (Å)	13.1629(2)
b (Å)	10.354(1)
c (Å)	17.2325(3)
β (degrees)	108.279(2)
volume (Å^3)	2230.00(6)
Z; calculated density (g × cm^{-3})	4; 1.755
μ (mm^{-1})	0.896
ϑ range for data collection (deg)	3.06−27.58
reflns collected/unique	41371/5134 [R(int) = 0.031]
data/params	5134/320
final R indices [$I > 2\sigma(I)$]	$R_1 = 0.0273$, w$R_2 = 0.0663$
R indices (all data)	$R_1 = 0.0351$, w$R_2 = 0.0677$
goodness of fit on F^2	1.014

Table 2. Selected Bond Lengths (Å) and Angles (deg) for $Co(hfa)_2 \cdot TMEDA$

Co−O(1)	2.061(1)	O(1)−Co−O(2)	86.76(4)
Co−O(2)	2.080(1)	O(3)−Co−O(4)	86.87(4)
Co−O(3)	2.087(1)	N(1)−Co−N(2)	84.33(4)
Co−O(4)	2.060(1)	O(1)−Co−O(4)	176.06(4)
Co−N(1)	2.159(1)	O(2)−Co−N(2)	175.76(4)
Co−N(2)	2.165(1)	O(3)−Co−N(1)	176.45(4)
N(1)−C(1)	1.484(2)	Co−O(1)−C(7)	125.11(9)
N(2)−C(2)	1.480(2)	Co−O(2)−C(9)	122.89(9)
O(1)−C(7)	1.251(2)	Co−O(3)−C(12)	122.98(9)
O(2)−C(9)	1.252(2)	Co−O(4)−C(14)	125.47(9)
O(3)−C(12)	1.249(2)	Co−N(1)−C(1)	104.58(8)
O(4)−C(14)	1.253(2)	Co−N(2)−C(2)	104.49(9)

possesses a *cis* geometry, with a hexacoordinated Co(II) center. The coordinating donor atoms are four oxygen atoms belonging to hfa ligands, plus two nitrogen atoms of the TMEDA molecule, resulting in a CoO_4N_2 *pseudo*-octahedral environment around Co. In fact, O−Co−O, N−Co−N, and O−Co−N bond angles (Table 2) point out to a certain distortion, within 4°, from an idealized octahedron.

The present structure is appreciably different from $Co(hfa)_2 \cdot 2H_2O \cdot CH_3(OCH_2CH_2)_4OCH_3$, in which the polyether moiety is not directly bonded to the Co(II) center but rather interacts with coordinated water through hydrogen bonds involving its O atoms, thus bridging the $Co(hfa)_2 \cdot 2H_2O$ units.[5] Conversely, the target product reported herein is completely solvent-free, despite its synthesis in an aqueous medium. This difference, which anticipates improved mass transport properties (see below), can be attributed to the fact that a diamine is a stronger Lewis base and competes more favorably with water than the polyether in the coordination of the metal center.[35]

In the crystal lattice of $Co(hfa)_2 \cdot TMEDA$, no intermolecular hydrogen bonds are present, implying an appreciable volatility for the adduct, a relevant feature in view of CVD/ALD application.[19] This characteristic can be traced back to the absence of water molecules in the crystalline structure and to the presence of fluorinated ligands, which are well-known to prevent H-bridge intermolecular interaction.[35] In a different way, for other Co(II) β-diketonates like the adducts of $Co(acac)_2$ with DMAPH, the occurrence of hydrogen bonding has been evidenced.[11]

The present bond lengths (see Table 2 for representative values) are consistent with the occurrence of strong metal−ligand interactions. The Co−O bond distances are in agreement with those found for Co(II)−hfa complexes (mean d(Co−O) = 2.050 Å) in the Cambridge Structural Database (CSD, version 5.25),[41] as well as with those reported for Co(II)−hfa polyether derivatives like $Co(hfa)_2 \cdot 2H_2O \cdot CH_3(OCH_2CH_2)_4OCH_3$ (d(Co−O) = 2.074 Å)[5] and $Co(hfa)_2 \cdot 2H_2O \cdot CH_3OCH_2CH_2OCH_3$ (d(Co−O) = 2.014 Å).[7]

It is also interesting to compare the metrical parameters of $Co(hfa)_2 \cdot TMEDA$ reported herein to those of the structurally similar compounds $Co(acac)_2 \cdot TMEDA$ and $Co(acac)_2 \cdot TEEDA$ (TEEDA= *N*,*N*,*N*′,*N*′-tetraethylethylenediamine), as well as with those of analogous $M(hfa)_2 \cdot TMEDA$ adducts previously characterized. Very similar d(Co−O) values have been reported (average = 2.064 and 2.054 Å) for $Co(acac)_2 \cdot TMEDA$ and $Co(acac)_2 \cdot TEEDA$ adducts, respectively, although the d(Co−N) values are higher in these cases with respect to $Co(hfa)_2 \cdot TMEDA$ (average = 2.228 and 2.262 Å, respectively, versus 2.162 Å in $Co(hfa)_2 \cdot TMEDA$; compare Table 2).[11,32] These differences highlight the role of the fluorinated hfa ligands with respect to the acac ones, increasing the Lewis acidity of the Co(II) center by electron-withdrawing effects and, in turn, strengthening its bonds with the ancillary diamine ligand, as already reported for Zn(β-diketonate)$_2 \cdot TMEDA$ compounds.[35]

In addition, in the present case, the Co−O bonds *trans* to the nitrogen atoms [Co−O(2), 2.080 Å, and Co−O(3), 2.087 Å] are slightly longer than those *trans* to the oxygen [Co−O(1), 2.061 Å, and Co−O(4), 2.060 Å]. A similar *trans* effect is in agreement with the results reported for other Co(β-diketonate)$_2 \cdot$diamine adducts,[11] as well as for $Mg(hfa)_2 \cdot TMEDA$ [$d(Mg-O)_{trans\text{-}O}$ = 2.043 Å; $d(Mg-O)_{trans\text{-}N}$ = 2.061 Å],[33] and $Zn(hfa)_2 \cdot TMEDA$ [$d(Zn-O)_{trans\text{-}O}$ = 2.100 Å; $d(Zn-O)_{trans\text{-}N}$ = 2.119 Å],[35] while it has not been reported for $Cd(hfa)_2 \cdot TMEDA$[38] and $Cu(hfa)_2 \cdot TMEDA$.[42] Among these compounds, $Mg(hfa)_2 \cdot TMEDA$ presents metal−oxygen distances very similar to those of $Co(hfa)_2 \cdot TMEDA$ (compare the above values with the ones in Table 2). As regards the O−Co−O an O−Co−N angular values (Table 2), they are in general agreement with those of $Co(acac)_2 \cdot TMEDA$[11] and $Zn(hfa)_2 \cdot TMEDA$.[35]

Chemical, Physical, and Mass Transport Properties of $Co(hfa)_2 \cdot TMEDA$. The complex FT-IR spectrum (Figure S1, Supporting Information) shows signals between 2800 and 3300 cm^{-1} (N−H, C−H, and N−CH_3 stretching),[5,7,30,43] and a broad band at ca. 3400 cm^{-1} due to adsorbed H_2O.[11,31] Peaks at 1645 and 1597 cm^{-1} (C=O and C=C stretching) and at 1410 and 1346 cm^{-1} (C−C and CF_3 stretching) are typical of coordinated hfa moieties.[5,7,11,30,31,43,44] Conversely, signals at 1260, 1188, and 1145 cm^{-1} can be ascribed to C−N

(41) Allen, F. H. *Acta Crystallogr., Sect. B* **2002**, *58*, 380.
(42) Delgado, S.; Muñoz, A.; Medina, M. E.; Pastor, C. J. *Inorg. Chim. Acta* **2006**, *359*, 109.
(43) Rao, C. N. R. *Chemical Applications of Infrared Spectroscopy*; Academic Press: London, 1963.
(44) Morris, M. L.; Moshier, R. W.; Sievers, R. E. *Inorg. Chem.* **1963**, *2*, 411.

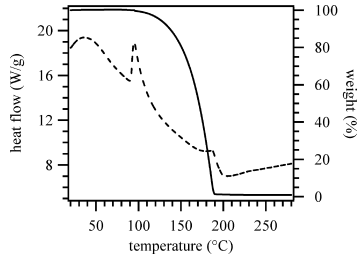

Figure 2. TG (solid line) and DSC (dotted line) profiles of the compound $Co(hfa)_2 \cdot TMEDA$ recorded under an air flow.

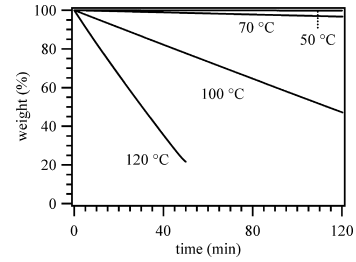

Figure 3. Isothermal weight loss studies for $Co(hfa)_2 \cdot TMEDA$ carried out at different temperatures.

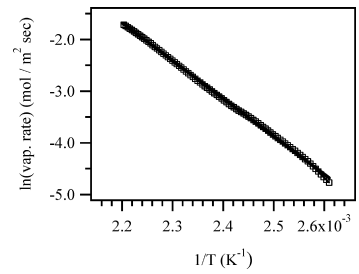

Figure 4. Arrhenius plot for the vaporization of $Co(hfa)_2 \cdot TMEDA$ under an air flow.

stretching in TMEDA,[43,44] whereas the peaks at 667 and 586 cm^{-1} can be related to Co−O and Co−N vibrations.[11]

The optical absorption spectrum of $Co(hfa)_2 \cdot TMEDA$ (Figure S2, Supporting Information) further supports the octahedral Co(II) coordination. The low-intensity vis band between 500 and 600 nm arises from the overlap of the $^4T_{1\ g}(F) \rightarrow {}^4T_{1g}(P)$ and $^4T_{1g}(F) \rightarrow {}^4A_{2g}(F)$ excitations,[30,45] while the signal at 420 nm can be ascribed to ligand−metal charge transfer.[10] In addition, the intense UV band at 303 nm is assigned to $\pi \rightarrow \pi^*$ intraligand transitions, without any significant metal center contribution.[46,47]

In order to examine the thermal behavior of the complex, thermal analyses were carried out under both inert (N_2) and oxidizing (synthetic air) flows. Irrespective of the adopted atmosphere, very similar results were obtained, thus indicating the occurrence of clean vaporization processes free from undesired side reactions in both cases. Figure 2 illustrates the TGA-DSC data for $Co(hfa)_2 \cdot TMEDA$ in the presence of oxygen, which is employed as a reactant gas even in CVD processes (see below). As can be noticed, the compound remained stable up to 120 °C and subsequently underwent a remarkable weight loss, associated with the powder vaporization in a single step. Remarkably, an almost zero constant weight residual was observed for $T > 190$ °C, suggesting a quantitative sublimation of the complex. In a different way, $Co(hfa)_2 \cdot 2H_2O$, $Co(hfa)_2 \cdot 2H_2O \cdot L$ with L = polyether, and $Co(acac)_2 \cdot TMEDA$ adducts possess a less favorable thermal behavior, being characterized by a broader weight loss at higher temperatures (i.e., a lower volatility),[5,6,31] along with a nonquantitative sublimation for the latter precursor.[11] The present favorable features can be related to the absence of H-bonding in $Co(hfa)_2 \cdot TMEDA$, as already discussed.

In agreement with the above findings, the DSC curve (Figure 2, dotted line) displayed two endothermic peaks located at 95 and 187 °C, respectively, associated with the adduct melting (see above) and subsequent vaporization, respectively.

Isothermal TG studies were carried out on $Co(hfa)_2 \cdot TMEDA$ at ambient pressure, and the results are displayed in Figure 3. The recorded curves revealed the compound sublimation at a constant and appreciable rate for long periods of time (>100 min in the temperature range 50−100 °C). Remarkably, the linear weight losses throughout the investigated temperature range are indicative of a pure vaporization, with no evidence of premature decomposition phenomena. This result is of considerable relevance for a CVD/ALD precursor, since it ensures reproducibility in constant vapor supply throughout the deposition process.

Figure 4 displays the logarithmic dependence of the vaporization rate, obtained by the TG profile derivative, on the inverse absolute temperature in the air. As can be noticed, a linear relationship is obtained, confirming the occurrence of clean vaporization processes with minimal side decomposition pathways. On the basis of the proportionality between the vaporization rate and the vapor pressure,[48] the logarithmic plot of the former versus the inverse absolute temperature enables evaluation of the apparent molar vaporization enthalpy from the curve slope on the basis of the Clausius−Clapeyron equation.[49] Irrespective of the adopted atmosphere (nitrogen or synthetic air), the calculation yielded $\Delta H = 60 \pm 1$ kJ mol^{-1}, a typical value for volatile CVD precursors.

Overall, thermal analyses indicate that $Co(hfa)_2 \cdot TMEDA$ is thermally stable and volatile, thus opening interesting perspectives for its subsequent application in CVD routes to cobalt oxide nanostructures.

Mass Spectrometry Investigation of $Co(hfa)_2 \cdot TMEDA$. Further information on the adduct behavior were gained by MS analyses and, in particular, by the use of ESI-MS. In fact, despite conventional electron ionization (EI)-MS seeming more appropriate for the investigation of CVD precursor reactivity, the more drastic ionization conditions might result in the destruction of particular ions diagnostic of the compound fragmentation. As a consequence, a softer ionization method like ESI represents the preferred choice.

(45) Bencini, A.; Benelli, C.; Gatteschi, D.; Zanchini, C. *Inorg. Chem.* **1983**, *22*, 2123.
(46) Nagashima, N.; Kudoh, S.; Nakata, M. *Chem. Phys. Lett.* **2003**, *374*, 59.
(47) Naik, M. B.; Gill, W. N.; Wentorf, R. H.; Reeves, R. R. *Thin Solid Films* **1995**, *262*, 60.
(48) Ashcroft, S. J. *Thermochim. Acta* **1971**, *2*, 512.
(49) Atkins, P. *Physical Chemistry*, 6th ed.; W. H. Freeman & Co. and Sumanas, Inc.: New York, 1998.

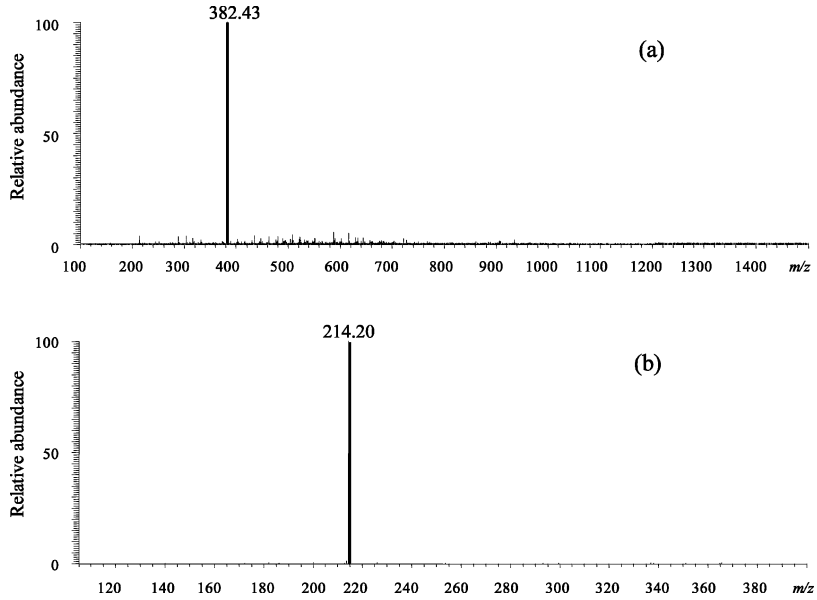

Figure 5. (a) Positive ion ESI-MS spectrum of a chloroform solution of $Co(hfa)_2 \cdot TMEDA$. (b) MS/MS spectra of the ions at *m*/*z* 382.43 in (a).

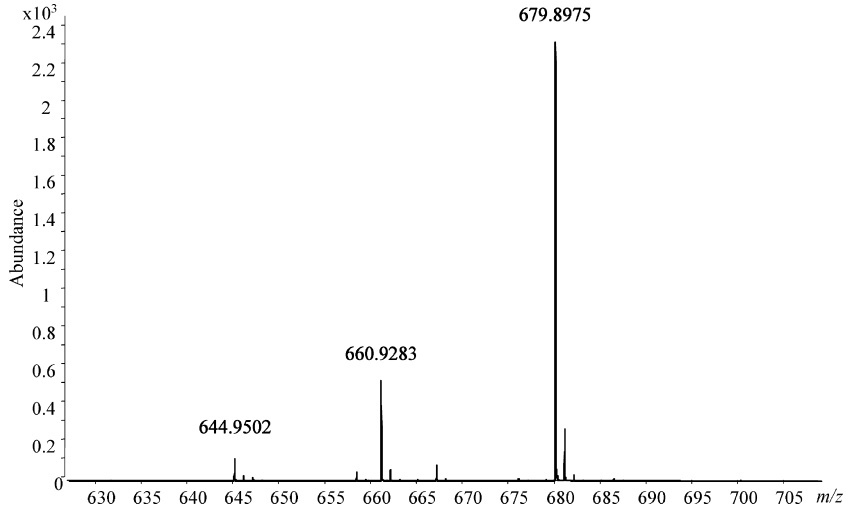

Figure 6. Negative ion ESI-MS spectrum of a methanolic solution of $Co(hfa)_2 \cdot TMEDA$ recorded using an Accurate-Mass 6520 Q-TOF instrument.

The positive ESI-MS spectrum from a chloroform solution (Figure 5a) was characterized by the ion at *m*/*z* 382, corresponding to $[Co(hfa) \cdot TMEDA]^+$. The related MS/MS spectrum (Figure 5b) revealed a very simple fragmentation of the above ion, since only the signal at *m*/*z* 214 was detected. On the basis of previous EI-MS studies on $Co(hfa)_2$ adducts reporting ligand-to-metal fluorine transfer,[6,7,31] a possible formula for this ion could be $[CoF_2 \cdot TMEDA + H]^+$. In negative ion mode (spectrum not reported), the only detected peak at *m*/*z* 207 was due to $[hfa]^-$ species. Conversely, in the ESI-MS analyses of $Co(hfa)_2 \cdot TMEDA$ solutions in CH_3OH and H_2O/CH_3OH, TMEDA-related signals were never detected, thus indicating a very rapid loss of the ancillary diamine ligand. In positive ion mode, no signals related to the complex were revealed, whereas in negative ion mode, three peaks at *m*/*z* 645, 661, and 680 could be detected. While the ion at *m*/*z* 680 corresponded to $[Co(hfa)_3]^-$, the identification of the negative ions at *m*/*z* 645 and 661 was not straightforward. In order to obtain their exact mass values and get further insight into their chemical nature, the methanolic solution of $Co(hfa)_2 \cdot TMEDA$ was analyzed by a Q-TOF instrument equipped with an ESI source. The resulting negative ion spectrum (Figure 6) enabled accurate measurment of the *m*/*z* values of the above ions as 644.9502, 660.9283, and 679.8975. As regards the latter, the calculated elemental formula was $C_{15}H_3O_6F_{18}Co$ (theoretical mass value, 679.8969; mass accuracy, 0.93 ppm), enabling its unambiguous attribution to $[Co(hfa)_3]^-$. In the MS/MS spectrum of ions at *m*/*z* 679.8975 (Figure 7a), only the signal at *m*/*z* 206.9886 was detected, corresponding to $[hfa]^-$ (theoretical mass value, 206.9875; mass accuracy, 5.3 ppm). Consequently, the ions at *m*/*z* 660.9283 and 644.9502 could not be considered as deriving from "in-source" fragmentation processes of $[Co(hfa)_3]^-$ (*m*/*z* 679.8975). The MS/MS spectra of these ions are shown in Figure 7b and c, respectively. Interestingly, in Figure 7b a low-abundance fragment at *m*/*z*472.9113 was detected (calculated formula, $C_{10}H_2O_4F_{12}Co$; theoretical mass value, 472.9088; mass accuracy, 5.3 ppm). This composition corresponded to a $[Co(hfa)_2]^-$ fragment, whose existence could be explained only by

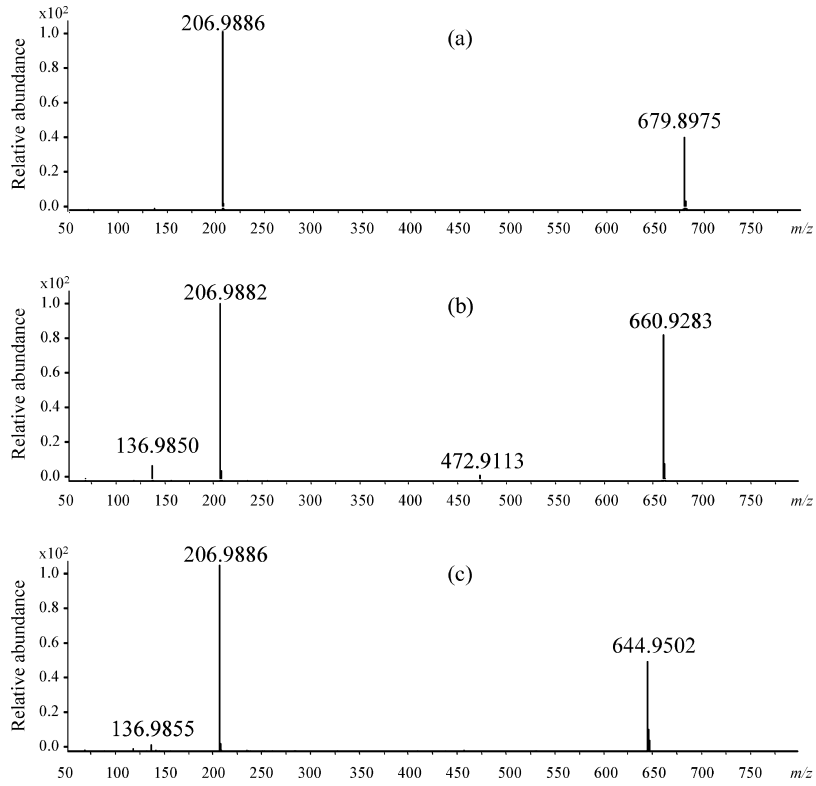

Figure 7. MS/MS spectra of the ions at *m/z* 679.8975 (a), *m/z* 660.9283 (b), and *m/z* 644.9502 (c), detected in the negative ion mode ESI-MS analysis of methanolic solutions of $Co(hfa)_2$·TMEDA. Spectra have been recorded by means of an Accurate-Mass 6520 Q-TOF instrument.

supposing the presence of a cobalt(I) center. As a consequence, a reduction from Co(II) (the original oxidation state in the precursor) to Co(I) seemed to take place under the adopted ESI conditions. This process could have occurred at the metal-solution interface of the ESI capillary in negative ion mode, owing to the high voltage differences existing between the ESI capillary and the counter-electrode in an ESI ion source.[50−52] It is worthwhile recalling that the electrospray source can be considered as a particular electrolytic cell, in which electrolysis maintains the charge balance, allowing the continuous production of charged droplets.[53,54] In addition, note that the Co(I) oxidation state is well-known and that various Co(I) complexes have been reported.[55] On this basis, a possible structure for the ion at *m/z* 660.9283 is $[Co(I)(hfa)_2(Hhfa\text{-}HF)]^-$ (elemental formula, $C_{15}H_3O_6F_{17}Co$; theoretical mass, 660.8985; mass accuracy, 41 ppm). Finally, the low-intensity peak at *m/z* 136.9850 was tentatively assigned to $[CF_3{-}CO{-}C{=}C{=}O]^-$, arising from the hfa moiety by means of a CHF_3 loss. The calculated elemental formula for the *m/z* 644.9502 ion is $C_{15}H_6O_6F_{16}Co$ (theoretical mass value, 644.92354; mass accuracy, 41 ppm), and a possible structure is $[Co(I)(hfa)_2(CF_2{=}(COH){-}CH_2{-}(COH){=}CF_2)]^-$, where the fragment $(CF_2{=}(COH){-}CH_2{-}(COH){=}CF_2)$ is likely derived from an hfa moiety. In the MS/MS spectrum of the ion at *m/z* 644.9502 (Figure 7c), apart from the signal at *m/z* 136.9855 (see above), the main peak at *m/z* 206.9886 was due to $[hfa]^-$, similarly to the case reported in Figure 7a.

Despite the above data pointing out to a sort of *solvent effect* in the ionization process, a common feature to all of the obtained ESI-MS and MS/MS spectra of $Co(hfa)_2$·TMEDA solutions was the presence of very few peaks, thus suggesting relatively simple fragmentation patterns. In addition, it is worth highlighting that no polynuclear species were ever detected, a promising feature for CVD/ALD processes.

CVD Depositions from $Co(hfa)_2$·TMEDA. A key point in the present study has been the precursor validation in CVD experiments aimed at the production of cobalt oxide nanosystems. The use of a vaporization temperature as low as 60 °C resulted in a reproducible and uniform mass supply, thus confirming the precursor volatility, as already highlighted by thermal analyses (see above). Note that the conventional $Co(dpm)_2$ precursor required a higher vaporization temperature under analogous CVD conditions.[10] Preliminary depositions in O_2 atmospheres on Si(100) substrates yielded uniform and crack-free samples, characterized by a bluish-gray color. GIXRD analyses (Figure 8) confirmed the presence of cubic Co_3O_4 as the only crystalline phase, as evidenced by the reflections at $2\vartheta = 31.2°$, 36.7°, and

(50) Kebarle, P.; Tang, L. *Anal. Chem.* **1993**, *65*, 972A.
(51) Van Berkel, G. J. In *Electrospray Ionization Mass Spectrometry: Fundamentals, Instrumentation and Applications*; Cole, R. B., Ed.; John Wiley & Sons: New York, 1997; pp 65−105.
(52) Van Berkel, G. J.; Zhou, F.; Aronson, J. T. *Int. J. Mass Spectrom. Ion Processes* **1997**, *162*, 55.
(53) Kebarle, P.; Ho, Y. In *Electrospray Ionization Mass Spectrometry: Fundamentals, Instrumentation and Applications*; Cole R. B., Ed.; John Wiley & Sons: New York, 1997; pp 3−63.
(54) Blades, A. T.; Ikonomou, M. G.; Kebarle, P. *Anal. Chem.* **1991**, *63*, 2109.
(55) Cotton, F. A.; Wilkinson, G. *Advanced Inorganic Chemistry*; John Wiley & Sons: New York, 1980, and references therein.

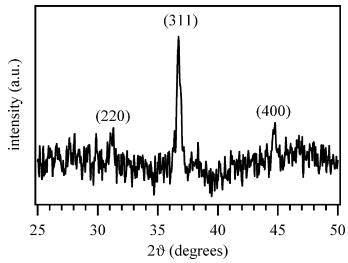

Figure 8. GIXRD patterns of a cobalt oxide sample deposited on Si(100) from $Co(hfa)_2 \cdot TMEDA$ at 400 °C.

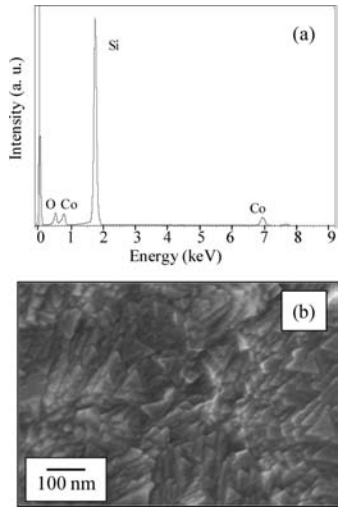

Figure 9. (a) EDX spectrum of a cobalt oxide specimen deposited on Si(100) at 400 °C. (b) Representative plane-view FE-SEM micrograph for the same system.

44.8°,[56] with no appreciable preferential orientations and a mean nanocrystal size of 25 nm. In agreement with structural results, the XPS Co $2p_{3/2}$ BE (780.5 eV, full width at half maximum = 3.8 eV), which did not show intense *shake-up* peaks, and the Auger parameter (1552.5 eV, calculated by the sum of the Co $2p_{3/2}$ BE and the CoLMM Auger peak kinetic energy) confirmed the presence of Co_3O_4,[10,57] with no appreciable fluorine contamination. The high purity of the obtained systems was testified by the disappearance of the carbon signals (≈20 atom % on the sample surface) upon a mild Ar^+ sputtering.

The high purity of the synthesized Co_3O_4 films has been further confirmed by EDXS analysis. The EDX spectrum of Figure 9a was characterized by peaks located at 0.528, 0.788, and 6.937 keV, attributable to OKα, CoLα, and CoKα transitions, respectively. The more intense signal at 1.748 keV was ascribed to the SiKα line of the substrate. The absence of contamination peaks pertaining to carbon or fluorine confirmed the clean decomposition pathway of the precursor, in agreement with the above analyses. Spectra recorded on different surface areas indicated an almost constant O/Co ratio of 1.32 ± 0.02, confirming the formation of Co_3O_4 with a uniform chemical composition. Finally, the FE-SEM micrograph reported in Figure 9b revealed a compact and very uniform morphology, characterized by well-interconnected triangular lamellar features with mean sizes ranging from 20 to 50 nm. Cross-sectional analyses allowed estimation of an average film thickness of 200 nm.

Conclusions

This study has proposed an efficient and low-cost synthetic strategy for the synthesis of $Co(hfa)_2 \cdot TMEDA$, a Co(II) β-diketonate adduct whose structure and chemico-physical characterization had never been reported previously. The target complex, obtained from commercially available products, is monomeric with a *cis pseudo*-octahedral arrangement of the ligands around a CoO_4N_2 core. In addition, it is characterized by a remarkable long-term stability and much lower air and moisture sensitivity compared to both Co(II) β-diketonate systems and homologous Co-hfa adducts. Thermal analyses have indicated that $Co(hfa)_2 \cdot TMEDA$ possesses an appreciable volatility and gives rise to vaporization processes free from premature decomposition. These favorable mass transport properties, along with the simple and relatively clean fragmentation pattern evidenced by MS analyses, demonstrate the great potential possessed by $Co(hfa)_2 \cdot TMEDA$ as a CVD/ALD precursor for cobalt oxide nanosystems, as confirmed by a preliminary CVD functional validation. Further experiments devoted to the interrelation between the Co−O nanosystem properties and the synthesis conditions are already under way, and the pertaining results will be the object of future investigation.

Acknowledgment. This work was financially supported by CNR-INSTM PROMO and the CARIPARO Foundation within the project "Multi-layer optical devices based on inorganic and hybrid materials by innovative synthetic strategies". Thanks are due to Mr. Loris Calore and Dr. Roberta Saini (Padova University) for elemental microanalyses and thermal analyses, respectively. Mr. Andrian Milanov (Bochum University) and Mr. Antonio Ravazzolo (Padova University) are also acknowledged for skilful technical assistance.

Supporting Information Available: X-ray crystallographic data of $Co(hfa)_2 \cdot TMEDA$ in the form of CIF file data. FT-IR and optical absorption spectra of $Co(hfa)_2 \cdot TMEDA$. This material is available free of charge via the Internet at http://pubs.acs.org.

IC801212V

(56) Pattern No. 36-1451, Joint Committee on Powder Diffraction Standards (JCPDS), 2000.

(57) Armelao, L.; Barreca, D.; Gross, S.; Tondello, E. *Surf. Sci. Spectra* **2001**, *8*, 14.